# Temporal Imaging of Incoherent-Light Intensity Waveforms Based on a Gated Time-Lens System

Bo Li
José Azaña

# Temporal Imaging of Incoherent-Light Intensity Waveforms Based on a Gated Time-Lens System

**Bo Li and José Azaña**

Institut National de la Recherche Scientifique—Energie, Matériaux et Télécommunications, Montréal, QC H5A 1K6, Canada

**Abstract:** We experimentally demonstrate temporal imaging of incoherent-light intensity waveforms using a combination of a temporal gating process and a time lens. This design allows one to set the system temporal field of view and resolution in an independent fashion, thus overcoming the intrinsic time–bandwidth product tradeoff of previous incoherent-light schemes based on the temporal pinhole camera concept. In a proof-of-concept experiment, we report incoherent-light temporal compression of intensity waveforms by a factor of 2.86, with a time–bandwidth product exceeding 300, i.e., resolution of ~26 ps (approximately fourfold improvement over the corresponding pinhole-only design) along a temporal field of view of ~8 ns, using a basic linear-optics setup.

**Index Terms:** Microwave photonics signal processing, imaging systems, incoherent sources, ultrafast measurements.

## 1. Introduction

Temporally incoherent light is intrinsically broadband and relatively easier to produce over large frequency bandwidths than its coherent counterpart (ultrashort optical pulses). As such, there is an increasing interest on the implementation of optical processing of high-speed time-domain signals using partially coherent or incoherent light waves [1]–[9], instead of the more conventional use of pulsed laser sources. Demonstrated functionalities using incoherent-light processing include arbitrary optical waveform generation [4], [5], ultrahigh dispersion of broadband radio-frequency (RF) signals [6], photonic temporal differentiation [7] and integration [8], etc.

On the other hand, temporal optical imaging is an important, general signal-processing concept, which can be used to enhance the time-bandwidth performance of systems devoted to the generation or measurement of high-frequency electronic and RF signals [10]–[12], or ultrafast optical information [13]–[20]. Recently, temporal imaging of incoherent-light waveforms has been demonstrated using a time-domain equivalent of a spatial pinhole camera [9]. The demonstrated scheme involves a combination of dispersion and temporal gating with a short pulse waveform (temporal pinhole [15]), and it has been shown to be particularly interesting to process RF waveforms over long temporal field of views, well into the nanosecond range [9]. Contrary to previous designs for imaging temporal RF waveforms [11], [12], the incoherent-light scheme

avoids the need for broadband pulsed laser sources [9]. However, as a critical practical limitation, the temporal pinhole camera exhibits a relatively *poor resolution*: well below the capabilities of previously reported time-lens systems [10]–[20]. Notice that resolutions have been achieved approaching 2 ps using linear time lenses based on electro-optics phase modulation [17]. The resolution constraint in a pinhole camera is associated with the fact that a shorter pinhole is needed for improved resolution, imposing challenging requirements on the temporal gating process. Notice also that the optimal pinhole duration depends on the dispersion values used in the system. Thus, additionally, the pinhole scheme exhibits an intrinsic design trade-off between the system's temporal field of view and resolution; a larger temporal field of view is achieved when the input dispersion is increased but this in turn deteriorates the system temporal resolution [9].

In the spatial-domain problem, it is well known that the use of a lens can improve the performance of the imaging system, particularly in terms of spatial resolution [21]. The same should be expected in regards to the time-domain problem. However, to the best of our knowledge, no temporal imaging system using a time lens has been previously demonstrated on incoherent-light waveforms. In this paper, we study and experimentally demonstrate a design for temporal imaging of incoherent-light intensity waveforms based on a gated time lens. The demonstrated scheme involves the use of a temporal pinhole coupled to a time lens process. Our work proves that this design combines the advantages of conventional temporal imaging based on time lens (*high resolution*) and incoherent-light temporal imaging based on a temporal pinhole (*large temporal field of view*). In particular, in the demonstrated design, the temporal resolution can be improved by increasing the temporal aperture of the time-lens process, i.e., duration of the preceding pinhole, without affecting the temporal field of view, which in turn depends on the product of the frequency bandwidth of the incoherent-light source and the input dispersion. We report here temporal imaging of incoherent-light intensity waveforms with a time-bandwidth product (TBP) exceeding 300, practically limited by our available linear-optics time-lens technology. Recall that the TBP, or number of processing points, is a widely used figure of merit for a temporal imaging system, and it is defined as the ratio between the system temporal field of view and its temporal resolution [20]. The demonstrated scheme should be particularly useful for generation, measurement and processing of high-speed intensity waveforms (e.g., RF signals) over long temporal windows.

## 2. Principle of Operation

An interesting observation is that the proposed scheme for incoherent-light temporal imaging can be interpreted as the time-domain equivalent of a human-eye imaging system. The latest is in fact an optimized design for imaging objects under incoherent light-wave illumination. To follow up with this equivalence, Fig. 1(a) illustrates the scheme of a human-eye optical-imaging system, which consists of a pupil and a crystalline lens. The pupil and the crystalline lens operate as a spatial pinhole and a spatial thin lens, respectively. The studied scheme for incoherent-light temporal imaging is shown in Fig. 1(b), where the dispersion, temporal pinhole and time lens are temporal equivalents of the diffraction process, pupil (spatial pinhole) and crystalline lens (spatial thin lens), respectively. In relation to Fig. 1(b) and (c), light from a broadband, temporally incoherent optical source is modulated in intensity by the input signal to be processed. The modulated light first propagates through a dispersive line, which provides a predominantly linear group-delay variation, with a slope $\ddot{\Phi}_{\text{In}}$, over the entire optical bandwidth. This is followed by temporal intensity modulation with a short pulse waveform, implementing the temporal pinhole. Subsequently, the modulated light is sent through a time lens, which imparts a quadratic phase across the temporal signal. Notice that the pinhole duration determines the time-lens aperture, or time span over which the phase modulation is imposed along the dispersed input waveform. The resulting light wave is finally dispersed through a second dispersive line, characterized by a linear group-delay with a slope $\ddot{\Phi}_{\text{Out}}$. As discussed below, the *averaged* optical
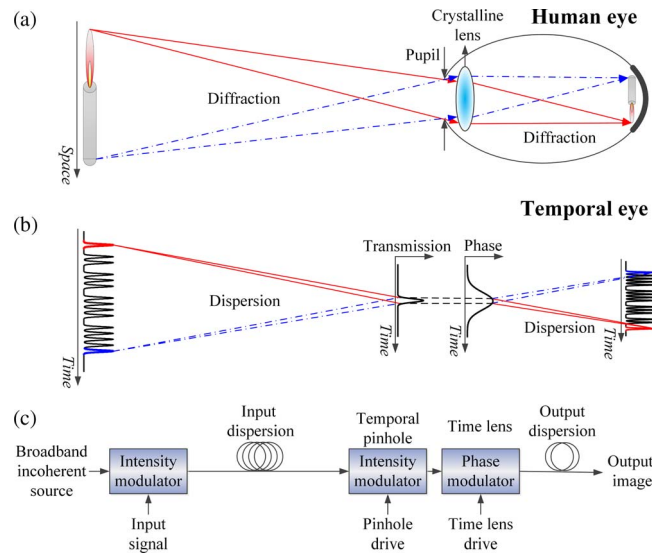
Fig. 1. Space–time equivalence for the incoherent-light lens-based temporal imaging design. (a) Imaging optics of a human eye system, based on spatial diffraction and a human eye, which consists of a pupil and a crystalline lens. (b) A lens-based temporal imaging system for incoherent light waves, which can be interpreted as a temporal counterpart of the human eye system. The dispersion, temporal pinhole, and time lens are temporal equivalents of the diffraction, pupil (spatial pinhole), and crystalline lens (spatial thin lens), respectively. (c) Block-diagram scheme of the time-lens-based temporal imaging system for incoherent-light waveforms.

intensity at the system output is a temporally scaled (magnified or compressed) image of the input intensity waveform, where the ratio between the output and input temporal scales, that is, the so-called temporal magnification factor, is given by $M = -\ddddot{\Phi}_{\text{Out}}/\ddddot{\Phi}_{\text{In}}$. "Averaged intensity" here refers to the averaging of the output intensity profiles for many different realizations of the same process.

Assuming a white-noise incoherent light source, the described scheme is linear in regards to averaged temporal intensity profiles [1], [22]. Under this assumption, the impulse response function of the considered incoherent-light temporal-imaging process can be obtained by squaring the magnitude of the field impulse response of the corresponding coherent system. In particular, we further assume that the well-known imaging condition is satisfied:

$$\frac{1}{\ddot{\Phi}_{\text{In}}} + \frac{1}{\ddot{\Phi}_{\text{Out}}} = \frac{1}{\ddot{\Phi}_{\text{TL},f}} \tag{1}$$

where $\ddot{\Phi}_{\text{TL},f}$ represents the focal group-delay dispersion of the time lens, i.e., the temporal quadratic phase introduced by the time lens is $\varphi_{\text{TL}}(\tau) = -\tau^2/(2\ddot{\Phi}_{\text{TL},f})$. In this case, it can be shown that the temporal impulse response of the proposed scheme under study performs the following operation:

$$\langle I_{\text{Out}}(\tau) \rangle \propto I_{\text{In}}\left(-\frac{\ddot{\Phi}_{\text{In}}}{\ddot{\Phi}_{\text{Out}}}\tau\right) \otimes \tilde{I}_{\text{Pinhole}}\left(\frac{1}{\ddot{\Phi}_{\text{Out}}}\tau\right) \tag{2}$$

where $\langle I_{\text{Out}}(\tau) \rangle$ holds for the averaged temporal intensity profile at the system output, $\otimes$ is for convolution, $I_{\text{In}}(\tau)$ is the temporal intensity profile of the input waveform, and $\tilde{I}_{\text{Pinhole}}(\omega)$ represents the Fourier transform of the temporal intensity profile of the temporal pinhole.

As shown by (2), the temporal intensity profile of the output waveform is, on average, a scaled (magnified or compressed) image of the input intensity waveform, with the anticipated
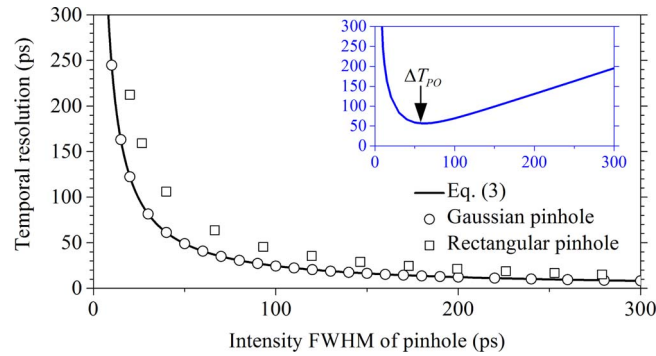
Fig. 2. Temporal resolution of an incoherent-light temporal imaging system based on a gated time lens. The inset plot shows the temporal resolution of a corresponding temporal pinhole system, which has the same configuration except that the time lens is removed [9].

magnification factor of $M = -\ddot{\Phi}_{Out}/\ddot{\Phi}_{In}$. The output temporal resolution of the system can be estimated as the intensity full width at half maximum (FWHM) of $\tilde{I}_{Pinhole}(\tau/\ddot{\Phi}_{Out})$, namely

$$\delta\tau_{Out} \approx \frac{(4\ln 2|\ddot{\Phi}_{Out}|)}{\Delta T_P} \tag{3}$$

where $\Delta T_P$ is the intensity FWHM of the temporal pinhole, assuming that the temporal pinhole has a Gaussian-like profile. Notice that this resolution is estimated under the assumption that the required quadratic phase modulation (time lens) can be induced over the entire temporal width of the pinhole, so that as mentioned above, the lens aperture is determined by the pinhole duration. The definition of resolution in (3) is the same as that for a conventional coherent temporal imaging system based on a time-lens process, essentially related to the frequency bandwidth swept by the time lens chirp along its time aperture [14], [23]. Fig. 2(a) shows the numerically simulated output temporal resolution of an *incoherent-light temporal compression* system (circles), assuming that the temporal pinhole has a Gaussian profile, the input dispersion is 1981 ps/nm, the output dispersion is −692 ps/nm, and the focal group-delay dispersion of the time lens is −1063.5 ps/nm (experimental specifications). In the numerical simulation, the output temporal resolution is estimated as the intensity FWHM of the time-domain impulse response, namely the time-domain pulse waveform at the system output when an ideal temporal impulse is launched at the system input. As shown in Fig. 2, there is an excellent agreement between the theoretical estimation [solid line, calculated based on (3)] and the results obtained by numerical simulations (circles). In addition, the numerically simulated temporal resolution for the proposed temporal imaging system with a rectangular temporal pinhole (squares) is also shown in Fig. 2. As predicted by (3), the temporal resolution can be made arbitrarily high simply by increasing the temporal pinhole duration, or the related time-lens bandwidth. This should be contrasted with the performance of a conventional temporal pinhole camera, where the resolution is optimized only for a very precise value of the pinhole duration $\Delta T_{PO}$, depending on the used dispersion values [9], [15], as shown in the inset plot of Fig. 2. Notice also that the temporal resolutions of these two systems are nearly the same when the temporal pinhole duration (lens aperture) is sufficiently short, i.e. $\leq \Delta T_{PO}$.

On the other hand, in a practical setup, the uniform (infinite-bandwidth) energy spectrum of the ideal white-noise light source is emulated over a limited frequency bandwidth, and this imposes a restriction on the system temporal field of view. As illustrated in Fig. 1(b), to ensure that some energy of the dispersed light pulse can pass through the pinhole, the input impulse must be within a certain time window, i.e., $T_A \approx 2\pi|\ddot{\Phi}_{in}|\Delta f_{Opt}$, where $\Delta f_{Opt}$ is the full-width optical bandwidth of the incoherent light source. The temporal field of view is the same as that of a conventional temporal pinhole camera [9], [15]. As anticipated, the temporal resolution can be
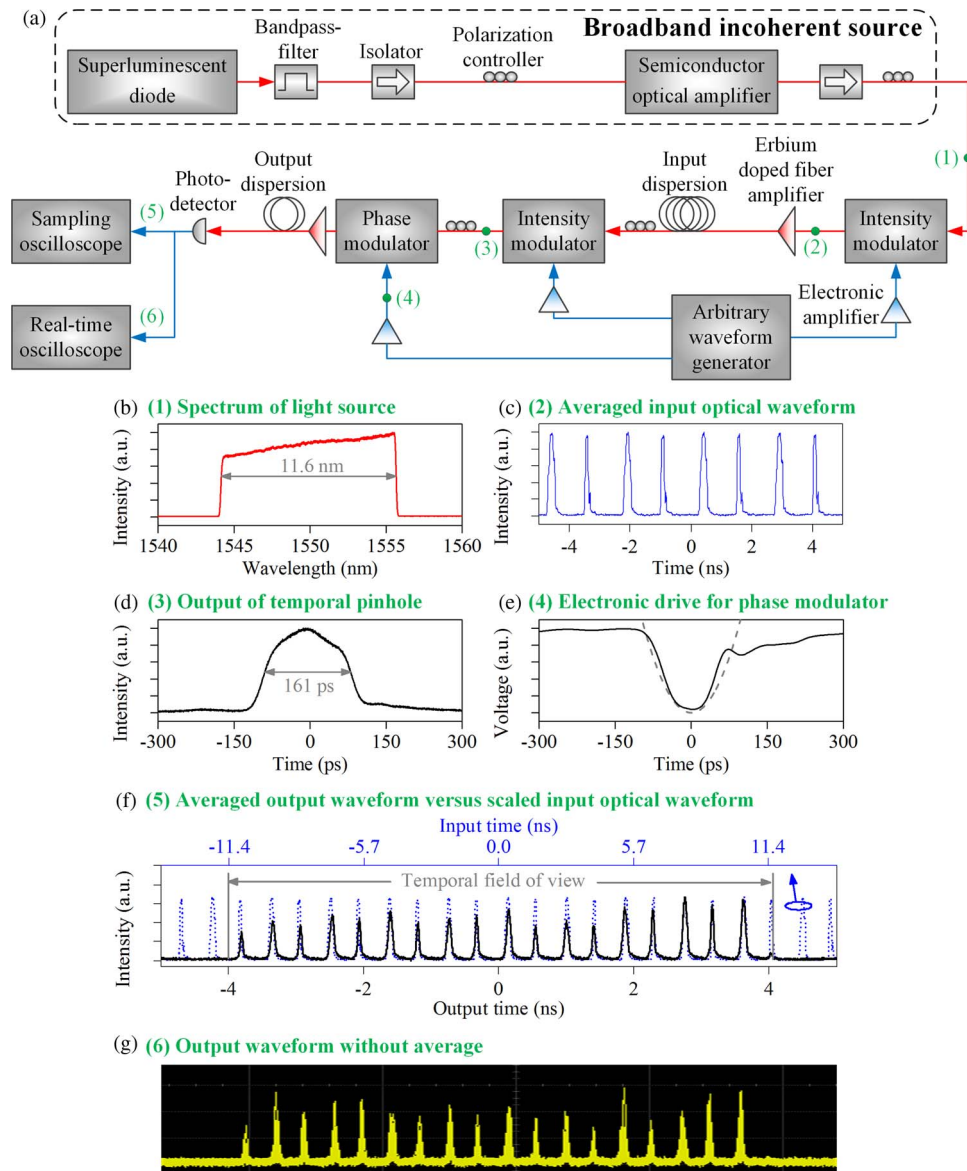
Fig. 3. Experimental setup results for the reported proof-of-concept experiments of an incoherent-light temporal imaging (compression) system based on a gated time lens. (a) Experimental configuration. (b) Spectrum of the broadband incoherent light source. (c) Input optical temporal waveform. (d) Optical output from the temporal pinhole. (e) Measured electronic drive (solid black) for phase modulation, compared with the theoretical profile (dashed gray). (f) Temporal intensity profile (solid black) of the output image compared with the scaled input temporal waveform (dashed blue), where the scaling between input time and output time is 2.86. All profiles in (c)–(f) are measured using a sampling oscilloscope and averaged 256 times. (g) Temporal intensity profile of the output image without averaging, which is measured by a real-time oscilloscope.

improved by increasing the lens aperture, i.e., pinhole duration, without affecting the temporal field of view.

## 3. Experimental Results

Fig. 3(a) shows the proof-of-concept experimental configuration and results for incoherent-light temporal compression of intensity (RF) signals based on the proposed temporal imaging
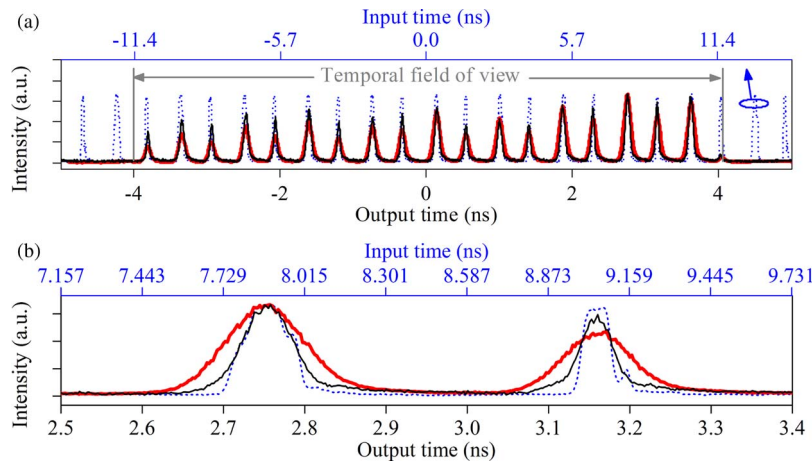
Fig. 4. Comparison of temporal-imaging results using the time-lens-based temporal imaging system (thin solid black) and a conventional temporal pinhole system (thick solid red) with the same specifications. (a) Temporal intensity profile of the output image compared with the scaled input temporal waveform (dashed blue), where the scaling between input time and output time is 2.86. (b) shows a closer view of (a).

scheme. Broadband incoherent light with a nearly uniform spectrum [~11.6 nm bandwidth and centered at a wavelength of 1549.9 nm, as shown in Fig. 3(b)] is first generated by spectrally filtering the optical radiation from a superluminescent diode followed by amplification with a semiconductor optical amplifier. The input incoherent optical signal to be imaged is obtained by intensity modulation of the incoherent light with the RF waveform under analysis using a 40-GHz electro-optic intensity modulator. The RF waveform is generated by a 12-Gsamples/s electronic arbitrary waveform generator and then amplified by a 12-GHz electronic amplifier. Fig. 3(c) shows an example of input temporal waveform, which is a periodic two-pulse sequence of Gaussian-like pulses. The two different consecutive pulses have FWHM of 214.7 ps and 108.8 ps, respectively, and their time separation is 1.17 ns. The modulated light is sent through the input dispersive line (dispersion $\approx$ 1981 ps/nm), and the time-domain pinhole, which is realized by another 40-GHz electro-optic intensity modulator driven by an electronic pulsed waveform, which is generated by the same arbitrary waveform generator and subsequently amplified by a 12.5-GHz electronic amplifier. Fig. 3(d) shows the measured averaged output of the temporal pinhole, which has a nearly Gaussian-like shape with an intensity FWHM of ~161 ps. As shown by Fig. 2, the temporal pinhole duration should be at least larger than $\triangle T_{PO}$, which is 61.6 ps for this particular setup so that the temporal resolution can be improved by the proposed temporal imaging system. After the temporal pinhole, the light is sent through an electro-optic phase modulator ($V_\pi \approx$ 3.9 V), which implements a time lens. The measured temporal waveform (solid black) of the electronic drive for the phase modulator is shown in Fig. 3(e), approaching the theoretical quadratic profile [dashed gray, calculated by (1)]. Finally, the modulated light is sent through the output dispersive line (dispersion $\approx$−692 ps/nm), and it is subsequently measured with a 45-GHz photo-detector attached to a 70-GHz sampling oscilloscope and a 28-GHz real-time oscilloscope. As shown in Fig. 3(e), the *averaged* output intensity waveform is a compressed temporal image of the input intensity waveform, with the expected compression factor of $C = 1/M \approx$ 2.86, along the 8-ns (23-ns) output (input) temporal field of view. Fig. 3(g) shows the temporal intensity profile of the output image without averaging.

To demonstrate the resolution improvement provided by the proposed temporal imaging system, Fig. 4 shows a comparison of the system's output image (thin solid black) with the output image from a temporal-pinhole-based system, not including the time lens (thick solid red). The temporal-pinhole-based system has the same configuration as the lens-based temporal imaging system shown in Fig. 3(a), except that the phase modulator is removed [9]. As shown

in Fig. 4(a), the lens-based temporal imaging system has the same temporal field of view as the pinhole-only system. However, the output image of the lens-based temporal imaging system exhibits a better agreement with the scaled input temporal waveform (dashed blue), as evidenced by the zoomed plot in Fig. 4(b). Recall again that the input waveform is a periodic two-pulse sequence of Gaussian-like pulses, represented in the plots with a dashed blue curve. In the output, the averaged intensity FWHM of the shortest pulses for the lens-based temporal imaging system and the pinhole-only system are, respectively, 46 ps and 103 ps, which, when compared with the scaled input FWHM of 38 ps, gives output resolutions of $\sqrt{46^2 - 38^2} \approx 25.9$ ps and $\sqrt{103^2 - 38^2} \approx 95.7$ ps, respectively [9], [18]. Even if the temporal pinhole duration would have been optimized for higher resolution, i.e., $\triangle T_{PO} \sim 61.6$ ps, the theoretically expected resolution ($\sim$56.44 ps) would still be poorer than the one reported here for the time-lens based scheme. However, in practice, the generation of the temporal pinhole duration with such a small time width, an arbitrary waveform generator with larger bandwidth will be required. Additionally, more energy will be filtered output when a narrower temporal pinhole is used. Notice that the temporal resolution of the demonstrated time-lens imaging system is slightly higher than the theoretical resolution of $\sim$15.2 ps, which may be mainly attributed to the deviation of the temporal phase modulation drive with respect to the ideal quadratic profile, as shown in Fig. 3(e). In addition, the limited bandwidth ($\sim$45 GHz) of the photo-detector also slightly contributes to the deviation. Based on the given estimates, a TBP of 308.9 is experimentally obtained.

Finally, it is important to note that the achieved resolution was ultimately limited by the specific electro-optic time lens used in our experiment. As shown in Fig. 3(e), the phase modulation amplitude implemented in our experiment is only $\sim 1.08\pi$; this could be improved to $\sim 10\pi$ using readily available electro-optic phase modulators, or even further to $> 100\pi$ by use of non-linear parametric time lenses [16], [18], leading to proportional improvements in the system temporal resolution.

## 4. Conclusion

In summary, we have proposed and demonstrated temporal imaging of incoherent-light intensity waveforms based on a temporally gated time-lens process. Experimental proof-of-concept experiments using a basic linear-optics configuration have shown a $\sim$4-fold improvement in temporal resolution over the equivalent temporal pinhole system, without affecting the intrinsic large aperture of the system. Further improvements should be readily possible by simply optimizing the time-lens process.

## References

[1] P. Naulleau and E. Leith, "Stretch, time lenses, and incoherent time imaging," *Appl. Opt.*, vol. 34, no. 20, pp. 4119–4128, Jul. 1995.

[2] C. Dorrer, "Temporal van Cittert–Zernike theorem and its application to the measurement of chromatic dispersion," *J. Opt. Soc. Amer. B, Opt. Phys.*, vol. 21, no. 8, pp. 1417–1423, Aug. 2004.

[3] H. Lajunen, J. Turunen, P. Vahimaa, J. Tervo, and F. Wyrowski, "Spectrally partially coherent pulse trains in dispersive media," *Opt. Commun.*, vol. 255, no. 1–3, pp. 12–22, Nov. 2005.

[4] V. Torres-Company, J. Lancis, and P. Andrés, "Incoherent frequency-to-time mapping: Application to incoherent pulse shaping," *J. Opt. Soc. Amer. A, Opt. Image Sci.*, vol. 24, no. 3, pp. 888–894, Mar. 2007.

[5] C. Dorrer, "Statistical analysis of incoherent pulse shaping," *Opt. Exp.*, vol. 17, no. 5, pp. 3341–3352, Mar. 2009.

[6] Y. Park and J. Azaña, "Ultrahigh dispersion of broadband microwave signals by incoherent photonic processing," *Opt. Exp.*, vol. 18, no. 14, pp. 14752–14761, Jul. 2010.

[7] A. Malacarne, R. Ashrafi, Y. Park, and J. Azaña, "Reconfigurable optical differential phase-shift-keying pattern recognition based on incoherent photonic processing," *Opt. Lett.*, vol. 36, no. 21, pp. 4290–4292, Nov. 2011.

[8] A. Malacarne *et al.*, "Single-shot photonic time-intensity integration based on a time-spectrum convolution system," *Opt. Lett.*, vol. 37, no. 8, pp. 1355–1357, Jan. 2012.

[9] B. Li and J. Azaña, "Incoherent-light temporal stretching of high-speed intensity waveforms," *Opt. Lett.*, vol. 39, no. 14, pp. 4243–4246, Jul. 2014.

[10] W. J. Caputi, "Stretch: A time-transformation technique," *IEEE Trans. Aerosp. Electron. Syst.*, vol. AES-7, no. 2, pp. 269–278, Mar. 1971.

[11] Y. Han and B. Jalali, "Photonic time-stretched analog-to-digital converter: Fundamental concepts and practical considerations," *J. Lightw. Tech.*, vol. 21, no. 12, pp. 3085–3103, Dec. 2003.

[12] J. Azaña, N. K. Berger, B. Levit, and B. Fischer, "Broadband arbitrary waveform generation based on microwave frequency upshifting in optical fibers," *J. Lightw. Tech.*, vol. 24, no. 7, pp. 2663–2675, Jul. 2006.

[13] E. Treacy, "Optical pulse compression with diffraction gratings," *IEEE J. Quantum Electron.*, vol. QE-5, no. 9, pp. 454–458, Sep. 1969.

[14] B. H. Kolner, "Space–time duality and the theory of temporal imaging," *IEEE J. Quantum Electron.*, vol. 30, no. 8, pp. 1951–1936, Aug. 1994.

[15] B. H. Kolner, "The pinhole time camera," *J. Opt. Soc. Amer. A, Opt. Image Sci.*, vol. 14, no. 12, pp. 3349–3357, Dec. 1997.

[16] C. V. Bennett and B. H. Kolner, "Principles of parametric temporal imaging. I. System configurations," *IEEE J. Quantum Electron.*, vol. 36, no. 4, pp. 430–437, Apr. 2000.

[17] J. van Howe, J. Hansryd, and C. Xu, "Multiwavelength pulse generator using time-lens compression," *Opt. Lett.*, vol. 29, no. 13, pp. 1470–1472, Jul. 2004.

[18] M. A. Foster *et al.*, "Silicon-chip-based ultrafast optical oscilloscope," *Nature*, vol. 456, no. 7218, pp. 81–84, Nov. 2008.

[19] M. Fridman, A. Farsi, Y. Okawachi, and A. L. Gaeta, "Demonstration of temporal cloaking," *Nature*, vol. 481, no. 7379, pp. 62–65, Jan. 2012.

[20] R. Salem, M. A. Foster, and A. L. Gaeta, "Application of space–time duality to ultrahigh-speed optical signal processing," *Adv. Opt. Photon.*, vol. 5, no. 3, pp. 274–317, Aug. 2013.

[21] B. E. Saleh and M. C. Teich, *Fundamentals of Photonics*. New York, NY, USA: Wiley, 1991, ch. 1.

[22] B. E. Saleh and M. C. Teich, *Fundamentals of Photonics*. New York, NY, USA: Wiley, 1991, ch. 10.

[23] B. H. Kolner, "Generalization of the concepts of focal length and f-number to space and time," *J. Opt. Soc. Amer. A, Opt. Image Sci.*, vol. 11, no. 12, pp. 3229–3234, Dec. 1994.